Journal of Crohn's and Colitis (2014) 8, 1710–1722

Available online at www.sciencedirect.com

ScienceDirect

Cigarette smoking is associated with intestinal barrier dysfunction in the small intestine but not in the large intestine of mice

Lugen Zuo[1], Yi Li[1], Honggang Wang, Rong Wu, Weiming Zhu*, Wei Zhang, Lei Cao, Lili Gu, Jianfeng Gong, Ning Li, Jieshou Li

Department of General Surgery, Jinling Hospital, Medical School of Nanjing University, Nanjing, China

Received 23 March 2014; received in revised form 23 July 2014; accepted 15 August 2014

KEYWORDS
Cigarette smoke;
Intestinal barrier;
Animal model;
Crohn's disease;
Ulcerative colitis

Abstract

Aims: To observe the effect of cigarette smoke (CS) on the small bowel and colon in mice and to attempt to explain the potential mechanisms that account for these effects.
Methods: Male BALB/c mice age 6–8 weeks were randomly divided into a CS group and a control group (n = 10 per group). CS mice were exposed to CS (five cigarettes each time, four times a day for 5 days a week using Hamburg II smoking machine and CS was diluted with air at a ratio of 1:6) for 10 weeks, and control mice were exposed to room air. After 10 weeks, mice were sacrificed for analysis (colon and small bowel).
Results: CS exposure impaired the intestinal barrier of the small bowel, based on evidence that CS mice exhibited increased intestinal permeability, bacterial translocation, intestinal villi atrophy, damaged tight junctions and abnormal tight junction proteins. These changes were partly mediated through the activated NF-κB (p65) signalling pathway. However, no obvious changes associated with the intestinal barrier were identified in the small bowel of control mice or the colons of control or CS mice.
Conclusions: CS is associated with intestinal barrier dysfunction in the small intestine but not in the large intestine of mice.

1. Introduction

Cigarette smoke (CS) remains the most widely studied and replicated environmental trigger for inflammatory bowel disease (IBD), including Crohn's disease (CD) and ulcerative

* Corresponding author at: Department of General surgery, Jinling Hospital, Medical School of Nanjing University, No. 305 East Zhongshan Road, Nanjing 210002, China. Tel./fax: +86 25 84806839.
E-mail address: dr_zhuweiming@126.com (W. Zhu).
[1] These authors contributed equally to this work.

http://dx.doi.org/10.1016/j.crohns.2014.08.008
1873-9946/

colitis (UC) [1]. CS is protective in UC with a lower incidence, better clinical course, and less need for surgery among smokers, but the opposite is true for CD [1,2]. However, the mechanisms for the differential effect on both diseases remain unclear. Attempts to account for the association between smoking and IBD have been hampered by the fact that the pathogenesis of both UC and CD remains unknown. One of the factors linking smoking and IBD might be intestinal permeability, which is considered to play a key role in the pathogenesis of both diseases [3,4] and can be influenced by CS [5,6]. However, the effects of smoking on intestinal permeability in patients with IBD and healthy volunteers are also controversial. Prytz et al. showed that smoking "tightens" the gut in healthy volunteers and suggested that a lower intestinal permeability in smokers might explain the protective effect of smoking in ulcerative colitis [7]. Suenaert et al. found that smoking could reduce the effect of NSAIDs on intestinal permeability, but no effect of smoking was observed on the baseline permeability of the small intestine in healthy volunteers [8]. However, in patients with ulcerative colitis, Benoni et al. demonstrated no difference in intestinal permeability between smokers and nonsmokers [9]. These studies failed to clarify the complexity of the impact of CS on intestinal permeability.

Although more attention has been paid to this issue, the underlying mechanism(s) of the dual effect of smoking on UC and CD still remained unclear [5,6]. In our study, we aimed to observe the impact of CS on the small bowel and colon in mice without a special genetic background and to attempt to account for the potential mechanism.

2. Materials and methods

2.1. Mice

Male BALB/c mice age 6–8 weeks and weighing 16–20 g were obtained from the Animal Center of Jin Ling Hospital. All mice were housed in plastic-bottomed wire-lidded cages and kept at 25 °C with a 12-h light/dark cycle. Mice had free access to water and were fed with a regular mouse chow. Body weight was measured at least once a week during the exposure period. The experimental procedures were performed in accordance with the Guidelines for Animal Experiments at Jin Ling Hospital and approved by the Ethics Committee of Jin Ling Hospital (Jiangsu, China).

2.2. Cigarette smoke exposure and experimental design

Mice were randomly divided into two groups (n = 10 per group). The first group was exposed to cigarette smoke for 10 weeks (CS), and the second group to room air for 10 weeks (Control). Considering the lifespan of a laboratory mouse, 10 weeks of smoking corresponds approximately to 10 years of smoking in humans [10]. Mice (CS group) were exposed to main stream as described previously [11,12]. Briefly, mice were exposed to the mainstream cigarette smoke of five cigarettes (Reference Cigarette 3R4F without filter; University of Kentucky, Lexington, KY, USA), four times a day with 30-minute smoke-free intervals, 5 days a week. The Hamburg II smoking machine (Borgwaldt KC, Hamburg, Germany) was used in our study, and puff duration and volume were 2 s and 35 ml, respectively. Cigarette smoke was diluted with air at a ratio of 1:6. Carboxyhaemoglobin in the sera of smoke-exposed mice reached a non-toxic level of 7.90 ± 0.28% (compared with 0.59 ± 0.21% in air-exposed mice), which is similar to blood concentrations of carboxyhaemoglobin in human smokers [13]. The levels of serum cotinine in CS mice were 150.50 ± 4.02 ng/ml (compared with less than 8 ng/ml in control mice), which is similar to that in human smoker [14]. Control group mice were exposed to filtered fresh air. Studies were performed 1–2 days after the last exposure to CS/air.

2.3. Levels of carboxyhaemoglobin and cotinine

Blood samples were collected from the caudal vein and stored at −80 °C for measurements of carboxyhaemoglobin and cotinine. The serum levels of carboxyhaemoglobin were measured using a blood gas analyser (Instrumentation Laboratory, Lexington, MA). Cotinine (nicotine metabolite) serum levels were determined using a cotinine assay kit (Orasure Technologies, Bethlehem, PA) in accordance with the manufacturer's recommendations.

2.4. Intestinal permeability in vivo

Mice were fasted for 4 h and then administered fluorescein isothiocyanate (FITC)-dextran (4 kDa; Sigma) by gavage at a dose of 600 $mg \cdot kg^{-1}$. After 4 h, the mice were killed by cervical dislocation and bled by cardiac puncture. Serum was isolated using centrifugation, and serum FITC levels were evaluated using fluorometry.

2.5. Analyse the permeability of colon and small bowel, respectively

The permeability of mouse intestines was measured by performing the Ussing Chamber Analyses as described in Ref. [15]. The colon and small bowel were removed from the animals and the luminal contents were gently rinsed out with PBS. Then, bowel segments were placed into oxygenated Krebs buffer (115 mM NaCl, 8 mM KCl, 1.25 mM $CaCl_2$, 1.2 mM $MgCl_2$, 2.0 mM $KHPO_4$, 25 mM $NaCO_3$, pH 7.33–7.37) at 37 °C. Small bowel sections were obtained proximal to the cecum, whereas large bowel sections were obtained proximal to the anus. Excised tissues were opened by dissection along the mesentery axis and mounted on 2.8 mm × 11.0 mm oblong sliders (Chamber Systems P2304; Warner Instruments, LLC, USA) with the luminal side down. The sliders were loaded into a four-chamber Ussing chamber system (Chamber Systems CSYS-4HA; Warner Instruments, LLC, USA) that was pre-calibrated. Krebs buffer was added to both chambers, whereas 10 mM glucose was added to the serosal side as an energy source and 10 mM mannitol was added to the luminal side to maintain osmotic balance. Agar-salt bridges were used to both monitor potential difference across the membrane and apply the appropriate short-circuit current (I_{sc}) to maintain the potential difference at zero as controlled through an automated voltage clamp. The system is controlled through the Acquire and Analyse software (Physiological Systems), which modulates

voltage and current controls remotely. The tissue was allowed to equilibrate for 15 min before I_{sc} readings were taken. In this way, we were able to measure transepithelial electric resistance (TEER) in intestinal epithelial tissues. After the tissues had equilibrated in the Ussing chamber, and baseline I_{sc} readings were acquired, 10^{-5} M horseradish peroxidase (HRP, Type VI; Sigma) was added to the luminal chambers to act as a probe for macromolecular permeability; 500 μL samples were taken from the serosal chambers at 30-min intervals for 2 h and replaced by 500 μL of fresh Krebs buffer to maintain constant volume. A modified Worthington method was used to evaluate the enzymatic activity of HRP in the serosal samples as described in Ref. [15].

2.6. Bacterial translocation

Using aseptic techniques, tissue samples from the mesenteric lymph nodes (MLN, two samples for each mouse) and caudal lymph nodes (CLN) were taken for bacteriological cultures. Collected tissue samples were weighed and 0.1 g of each tissues was homogenised in a tissue grinder with 0.9 ml sterile saline. The homogenates were diluted and 100 μl dilutions were taken and cultured on Mac–Conkey's agar (Sigma) at 37 °C for 24 h. Bacterial growth in the plates was expressed as colony-forming units/g of tissue. The result of cultures was considered to be positive when more than 10^2 colonies/g of tissue were found [16].

2.7. Histological examinations

Histologic evaluation was performed in H&E-stained sections of the colon (distal colon and proximal colon) and small bowel (distal small bowel and proximal small bowel) tissues fixed in 10% formalin solution. Slides were reviewed in a blinded fashion and assessed according to a previously validated intestinal histologic inflammatory score with a range from 0 to 9.[17] Briefly, histologic indices were evaluated for the presence of (1) active inflammation (infiltration with neutrophils), (2) chronic inflammation (lymphocytes, plasma cells, and macrophages in the mucosa and submucosa), and (3) villus distortion (flattening and/or widening of normal villus architecture). For each index, a score ranging from 0 (normal histology) to 3 (maximum severity of histologic changes) was applied. The sum of all 3 individual components was expressed as the total inflammatory score. Peyer's patches were not included in the calculation.

2.8. Transmission electron microscopy of tight junctions

Sections of the colon and small bowel (2 mm) were fixed for 2 h in 4% buffered glutaraldehyde. The sections were cut into smaller pieces, post-fixed in 1% osmium tetroxide (OsO_4), sequentially dehydrated through graded alcohols, infiltrated through Epon 812 and then embedded in resin. Thin sections were cut and stained with uranyl acetate and lead citrate, and examined with a Hitachi H-600 transmission electron microscope (Hitachi) operated at 75 kV at a magnification of 20,000×. Tight junctions were considered to have increased permeability when the electron-dense marker penetrated into the junctional complex.

2.9. Immunofluorescence assessment of tight junction proteins

The localisation of zona occludens-1 (ZO-1), occludin, claudin-1 proteins and NF-κB-p65 was determined by immunofluorescence as described in Ref. [18]. The intestine segments were immediately removed, washed with PBS, mounted in embedding medium, and stored at −80 °C until use. Frozen sections were cut at 10 μm, and mounted on the slides. The nonspecific background was blocked by incubation with 5% bovine serum albumin plus 5% newborn bovine serum in PBS for 30 min at room temperature. The sections were incubated with rabbit polyclonal antibody against ZO-1 (Abcam), rabbit polyclonal antibodies against occluding (Abcam), rabbit polyclonal antibody against claudin-1 (Abcam) and NF-κB-p65 (Santa Cruz Biotechnology) at 4 °C overnight. The sections were probed with their respective FITC-conjugated secondary IgG antibodies. The nuclei were counterstained with DAPI (4, 6-diamidino-2-phenylindole). Slides incubated without any primary antibody were used as negative controls. Confocal analysis was performed with a confocal scanning microscope (Leica Microsystems, Heidelberg GmbH, Mannheim, Germany).

2.10. Enzyme-linked immunosorbent assay

The intestinal levels of TNF-α and IL-1β were determined by enzyme-linked immunosorbent assay (ELISA). Briefly, the intestinal mucosa tissue of the small bowel and colon were removed and stored at −80 °C until use (also for quantitative real-time PCR and Western blot analysis). When ELISA was performed, the tissues were homogenised in 1 ml of Tris–HCl buffer containing protease inhibitors (Sigma). Then, the samples were centrifuged at 3000 rpm at 4 °C for 30 min, and the supernatant was frozen at −80 °C until assay. The protein concentration was determined by the Bradford assay. The levels of TNF-α and IL-1β (pg/mg) were measured using commercial ELISA kits (R&D) according to the manufacturer's instructions.

2.11. Quantitative real-time PCR analysis

The mRNA levels of TNF-α, IL-1β, defensin-α4, heat shock protein 70 (HSP 70), high mobility group box 1 (HMGB1), cytochrome P450 1A1 (CYP450 1A1) and heme oxygenase-1 (HO-1) were measured by quantitative real-time PCR analysis as described in Refs. [19–21]. Briefly, after total RNA was extracted from intestinal mucosa tissues using TRIZOL reagent (Life Technologies Inc.), the oligo (dT)-primed complementary DNA was used for reverse transcription of purified RNA. The amount of transcript of the genes of interest was measured by real-time quantitative RT-PCR assay using SYBR Green detection (Applied Biosystems, Carlsbad, CA). All reactions were independently repeated at least twice to ensure the reproducibility of the results. Primer sequences are listed in Table 1. Expression levels of each gene were normalised using β-actin gene expression, yielding the relative expression value.

Table 1 Primer sequences.

TNF-α	Forward	CCCAGACCCTCACACTCAGATC
	Reverse	CCTCCACTTGGTGGTTTGCTAC
IL-1β	Forward	AAGTGGTGTTCTGCATGAGC
	Reverse	TGAGAAGTGCTGATGTACCA
HSP70	Forward	ACCAGCCTTCCCCAGAGCAT
	Reverse	TCTGCTTCTGGAAGGCTGC
HMGB1	Forward	GCTGACAAGGCTCGTTATGAA
	Reverse	CCTTTGATTTTGGGGCGGTA
HO-1	Forward	CGTGCTCGAATGAACACTCT
	Reverse	GCTCCTCAAACAGCTCAATG
CYP450 1A1	Forward	CAATGAGTTTGGGGAGGTTACTG
	Reverse	CCCTTCTCAAATGTCCTGTAGTG
Defensin α 4	Forward	CCAGGGGAAGATGACCAGGCTG
	Reverse	TGCAGCGACGATTTCTACAAAGGC
β-actin	Forward	TGGAATCCTGTGGCATCCATGAAAC
	Reverse	TAAAACGCAGCTCAGTAACAGTCCG

2.12. Western blot analysis

Whole-cell protein extraction and nuclear protein from the intestinal mucosa of small bowel and colon were prepared as previously described [22]. Western blot analysis was conducted as described in Ref. [23]. Briefly, protein extracts from the intestinal mucosa of the small bowel and colon were separated by 10% sodium dodecyl sulphate polyacrylamide gel electrophoresis (SDS-PAGE) gradient gels and transferred to nitrocellulose membranes for immunoblotting analyses. The primary antibodies were 1:1000 dilutions of rabbit polyclonal antibody against p65, p-p65, p-IKK, p-I κB, ZO-1, occludin, claudin-1, CYP450 1A1 and Histone$_3$ (H_3) or β-actin (Cell Signalling). Western blot analyses were performed with horseradish peroxidase (HRP)-conjugated secondary antibody (1:2000 dilution, Cell Signalling) using enhanced chemiluminescence Western blotting detection reagents (Amersham, Arlington Heights, IL, USA). Quantification was performed by optical density methods using the ImageJ software. The results are expressed as relative density to β-actin or H_3, normalised to the mean value of the control group [19].

2.13. Statistical analysis

All data analysis was performed using Statistical Package for Social Sciences (SPSS Inc., Chicago, IL, USA) software version 19.0. Continuous, normally distributed data are presented as the mean ± standard error (mean ± SEM). We used unpaired t-tests to compare parametric continuous variables. Binary and categorical data were compared by means of chi-squared tests for contingency tables. Fisher's exact test was performed when cases ≤5. A level of $P < 0.05$ was considered statistically significant.

3. Results

3.1. CS exposure caused a slower rate of weight gain

The most obvious change caused by CS exposure was the change in the body weight of the two groups. As presented in Fig. 1, the body weight increased steadily in all groups throughout the study. However, the rate of increase was slower in the CS group than in the control group. CS mice had lower average body weight than control mice from week 3 to week 10 ($P < 0.01$).

3.2. CS exposure increased intestinal permeability in the small bowel

Intestinal permeability was measured in vivo. As shown in Fig. 2(A), CS mice had higher levels of serum dextran conjugates compared to control mice ($P < 0.01$). We also analysed the permeability of the colon and small bowel in an Ussing Chamber in vitro. CS mice showed decreased resistance in the small bowel but not the colon when compared to control mice ($P < 0.05$; Fig. 2B). There was no significant difference in colon permeability between the two groups, but the small bowel from CS mice showed a significant increase in permeability compared with that of control mice ($P < 0.01$; Fig. 2C). These data indicated that CS exposure can increase the permeability of the small bowel.

3.3. CS exposure led to bacterial translocation

In view of our results showing that CS exposure can increase intestinal permeability, this change may lead to bacterial translocation known to play an important role in the aetiology of human inflammatory bowel diseases [4]. Bacterial culture of mesenteric lymph node (MLN) and caudal lymph node (CLN) were performed as shown in Fig. 2D. The rate of bacterial translocation of the MLN was higher in CS mice compared with control mice. No significant difference was found between the two groups in the rate of bacterial translocation of the CLN. This finding combined with the above results demonstrated that intestinal barrier dysfunction can be caused by CS exposure. Interestingly, only the small bowel was involved. It appeared as though the colon had the capacity to stay injury-free. To decipher the cause, further studies were performed as follows.

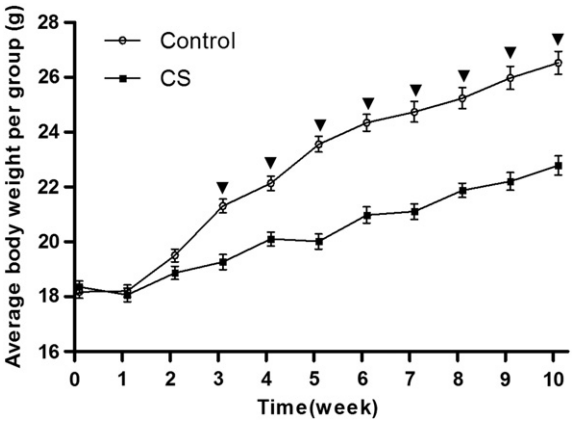

Figure 1 CS exposure caused a slower rate of weight gain. CS-exposed animals grew at a slower rate compared to control mice. Data are expressed as the mean ± SEM (n = 10 per group). ▼$P < 0.01$ versus CS group.

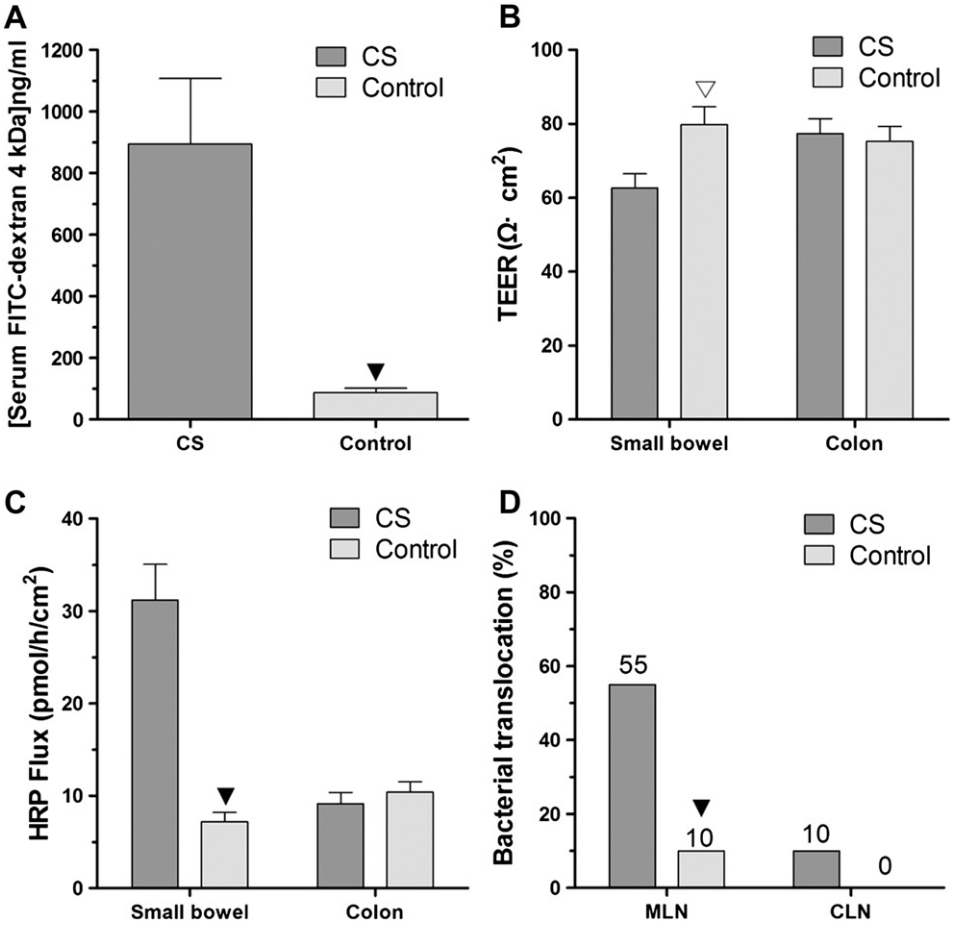

Figure 2 CS exposure increased intestinal permeability in the small bowel but not in the colon. CS mice had higher serum levels of dextran conjugate compared to control mice (A). CS mice showed decreased resistance in the small bowel but not the colon compared with control mice (B). No significant difference was noted in the colon permeability between the two groups, but the small bowel of CS mice showed a significant increase in intestinal permeability compared with control mice (C). The rate of bacterial translocation of the MLN was higher in CS mice compared with control mice (D). MLN, mesenteric lymph node; CLN, caudal lymph node. Data are expressed as the mean ± SEM (n = 10 per group). $^{\triangledown}P < 0.05$ versus CS group. $^{\blacktriangledown}P < 0.01$ versus CS group.

3.4. CS exposure altered the microscopic structure of small bowel villi

The histological examinations of the two groups of mice are shown in Fig. 3. The microscopic structure of the small bowel villi (including the distal small bowel and proximal small bowel) of CS mice was altered, and characterised by impaired intestinal villus structure, decreased number of intestinal villi and accumulation of inflammatory cells in the lamina propria. CS mice had a higher small bowel histologic score (including the distal small bowel and proximal small bowel) than control group, the difference was statistically significant ($P < 0.01$; Fig. 3B). There was no significant difference in the colon histologic score (including the distal colon and proximal colon) between the two groups (Fig. 3D). As shown in Fig. 3E, hypertrophy of Peyer's patches was observed in the small bowel from CS mice (occurrence rate was 9/10), but not in control mice (figures not shown). This finding was consistent with the results of Verschuere, et al. [12]. No obvious change was found in the structure of Paneth cells from the two groups. As no obvious difference between the histologic scores of the distal and proximal intestines (small bowel or larger bowel) was found, we chose the distal small bowel and distal larger bowel as representative segments of the small bowel or large bowel for further analysis.

3.5. CS exposure damaged the morphology of tight junctions in the small bowel

The presence of impaired small bowel villi caused by CS was verified by microscopy (H&E). We also investigated the change in intestinal villus structure at the submicroscopic level to observe the morphology of tight junctions (TJ). When transmission electron microscopy analysis was performed to investigate the intestinal villi, we found that the ultrastructural morphology of TJ in the small bowel villi was altered by CS exposure. As demonstrated in Fig. 4A, decreased amounts of electron-dense materials in the TJ and abnormal desmosomes were found in the small bowel villi of CS mice. The TJ and desmosomes were intact in the

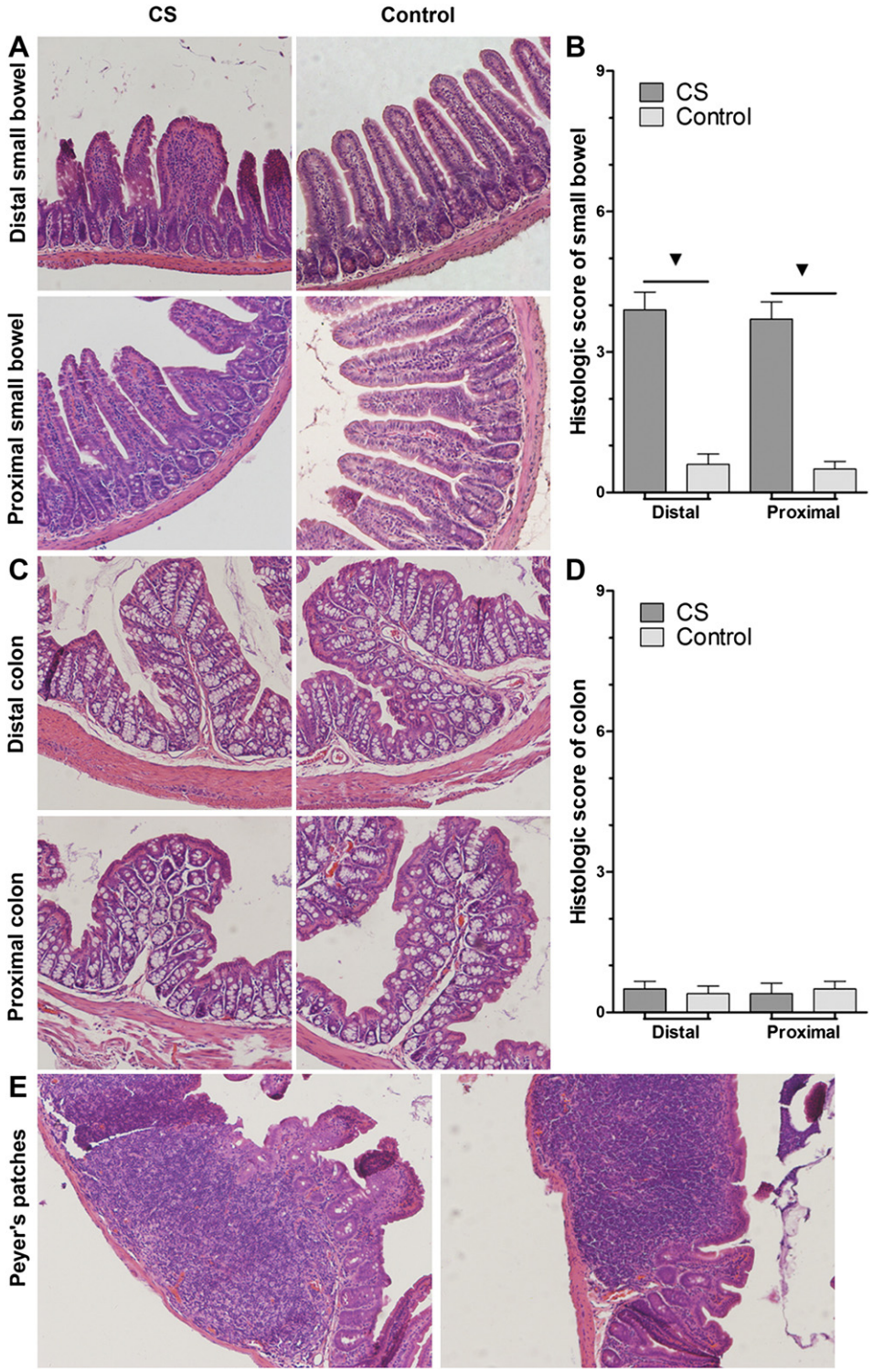

Figure 3 The microscopic structure of small bowel villi was altered by CS exposure (H&E, ×100). (A) In a small bowel from a CS mouse (including distal and proximal small bowel), the microscopic structure of intestinal villi was altered, and characterised by impaired intestinal villus structure, decreased number of intestinal villi and accumulation of inflammatory cells in the lamina propria. (B) CS mice had higher histologic scores in the distal small bowel and proximal small bowel than those of the control group ($P < 0.01$). (C) No obvious abnormality was detected in the colon (including distal colon and proximal colon) in both groups. (D) There was no significant difference in the colon histologic score between the two groups. (E) Hypertrophy of Peyer's patches was found in the small bowel of CS mice, but not in control mice (data not shown). CS, CS group; control, control group. Data are expressed as the mean ± SEM (n = 10 per group). $^{\blacktriangledown}P < 0.01$ versus CS group.

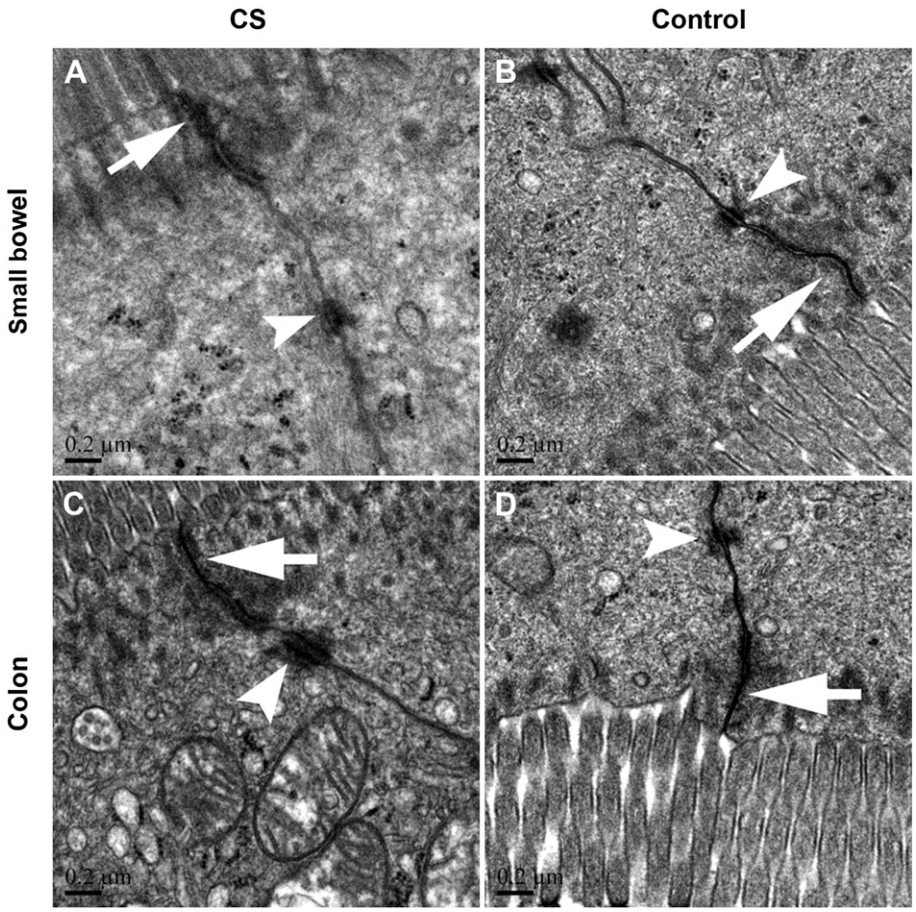

Figure 4 CS exposure damaged the morphology of TJ in the small bowel but not the colon (n = 10 per group). (A) In the small bowel in the CS group, the tight junction (TJ) ultrastructure was altered, and characterised by decreased electron-dense materials in the TJ and abnormal desmosomes. The TJ and desmosomes were intact in the small bowel of control mice (B) and the colon of both CS (C) and control mice (D). Arrows, tight junctions, arrow heads, and desmosomes. Scale bars = 0.2 μm.

small bowel of control mice (Fig. 4B) and in the colons of both CS (Fig. 4C) and control mice (Fig. 4D).

3.6. CS exposure altered the small bowel epithelium tight junction proteins

As tight junction proteins (including claudin-1, occludin and ZO-1) contributed to the barrier function, redistribution of those proteins led to altered TJ structure. Thus, immunofluorescence technique was used to evaluate the intestinal mucosal at the molecular level, and the results are shown in Fig. 5. We found that biotin staining (claudin-1, occludin and ZO-1), ectopic to the lamina propria or deep into the epithelial surface and some of the surface of villi, lacked focused staining in the small bowel of CS mice whereas the distribution and density of focused staining were normal in the small bowel of control mice (Fig. 5A–C) and in the colons of both CS and control mice (Fig. 5D–F). As shown in Fig. 6, the concentration of claudin-1, occludin and ZO-1 in the small bowel mucosa of CS mice was found to be significantly lower when compared to those of control mice. No significant difference in colonic mucosa claudins was found between the two groups. This result combined with above findings indicated that CS exposure can cause damage to the intestinal barrier structure, which contributed to intestinal barrier dysfunction. However, the molecular mechanism still remains unknown.

3.7. CS induced NF-κB activation in the small bowel

Intestinal inflammatory factors and stress response markers were examined to identify the possible mechanism of intestinal barrier dysfunction caused by CS exposure. The mRNA of defensin-α4, HO-1, and HSP 70 was compared between the two groups (small bowel and colon) but no significant difference was found (Fig. 7A–C). The CS mice had a higher level of HMGB1 mRNA in the small bowel than that of control group (Fig. 7D). CS exposure significantly elevated the concentration of TNF-α protein in the small bowel of CS mice compared to that of control mice (Fig. 7E), which was confirmed by the assessment of TNF-α mRNA expression (Fig. 7F). The concentration of IL-1β protein in the small bowel of CS mice was also found to be significantly increased compared to control mice

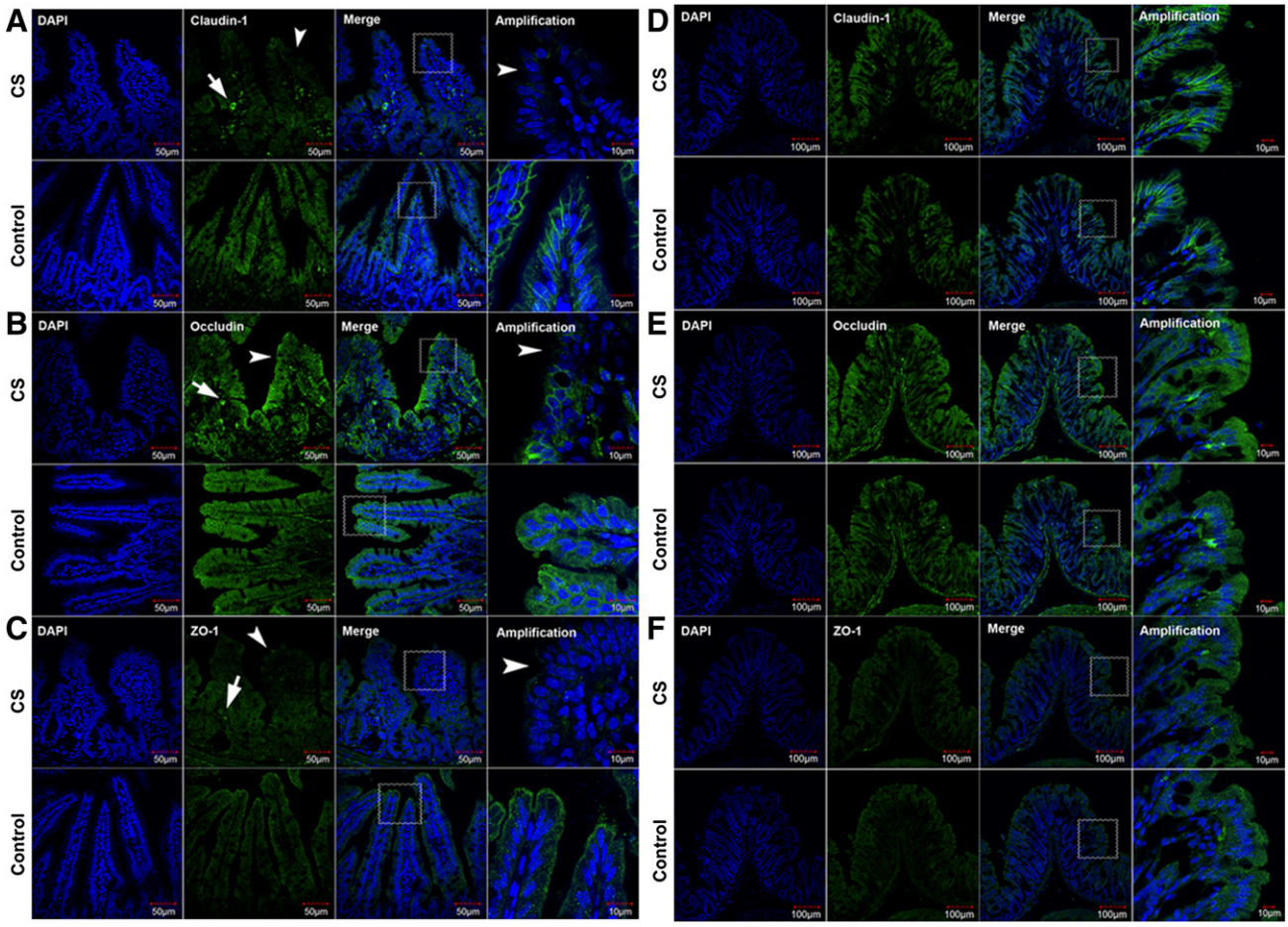

Figure 5 Localisation of ZO-1, occludin and claudin-1 and DAPI (DNA) on sections of the small bowel from the two groups (A–C; n = 10 per group). Tight junction proteins (green, including ZO-1, occludin and claudin-1) and DAPI staining (blue), merged tight junction protein and DAPI, as well as amplified merged tight junction protein and DAPI images are presented. Arrows indicated that biotin staining was ectopic to the lamina propria or deep into the epithelial surface. Arrowheads indicated the lack of focused staining in the surface of villi. Abnormal claudins were found only in the small bowel of CS mice whereas the distribution and density of focused staining were nearly normal in the small bowel of control mice and colon of the two groups (D–F).

(Fig. 7G); however, this finding was not confirmed by the quantitative mRNA analysis (Fig. 7H; $P = 0.087$). There was no significant difference of CYP450 1A1 on the protein and mRNA level between the two groups (Fig. 7I–J). As the expression of TNF-α, IL-1β and HMGB1 can be mediated by the NF-kappaB (NF-κB) signalling pathway [24], this pathway may also be activated by CS exposure. This hypothesis was verified as shown in Fig. 8. The non-phosphorylated (Fig. 8A) and phosphorylated (Fig. 8B) forms of NF-κB p65 were all increased in the small bowel of CS mice compared to control mice. The p-IKK and p-I κB were also increased in the small bowel of CS mice (Fig. 8C). Consistent with the results of immunofluorescence staining, we observed that the nuclear expression of NF-κB was markedly increased in the small bowel of CS mice (Fig. 8D). However, no significant difference in the expression of NF-κB was detected in the colon of these two groups. These results indicated intestinal barrier dysfunction caused by CS exposure, at least, partly through activation of the NF-κB signalling pathway.

4. Discussion

To the best of our knowledge, this study is the first to examine the effects of CS on intestinal barrier function in both the small bowel and colon, using mice without special genetic background and extraneous stimulus. Our main findings can be summarised as follows: 1) CS exposure can cause intestinal barrier dysfunction of the small bowel with increased intestinal permeability and bacterial translocation; 2) the structure of small bowel epithelial barrier can be injured by CS exposure, which can contribute to intestinal barrier dysfunction; 3) the NF-κB signalling pathway can be activated in the small bowel by CS exposure, which may be partly responsible for damage to the intestinal barrier structure. Indeed, it is a very interesting phenomenon that under the same CS stimulus, only the small bowel was involved while no obvious changes could be found in the colon.

Our data showed that the small bowel of CS mice had high levels of TNF-α, IL-1β and HMGB1 expression that could

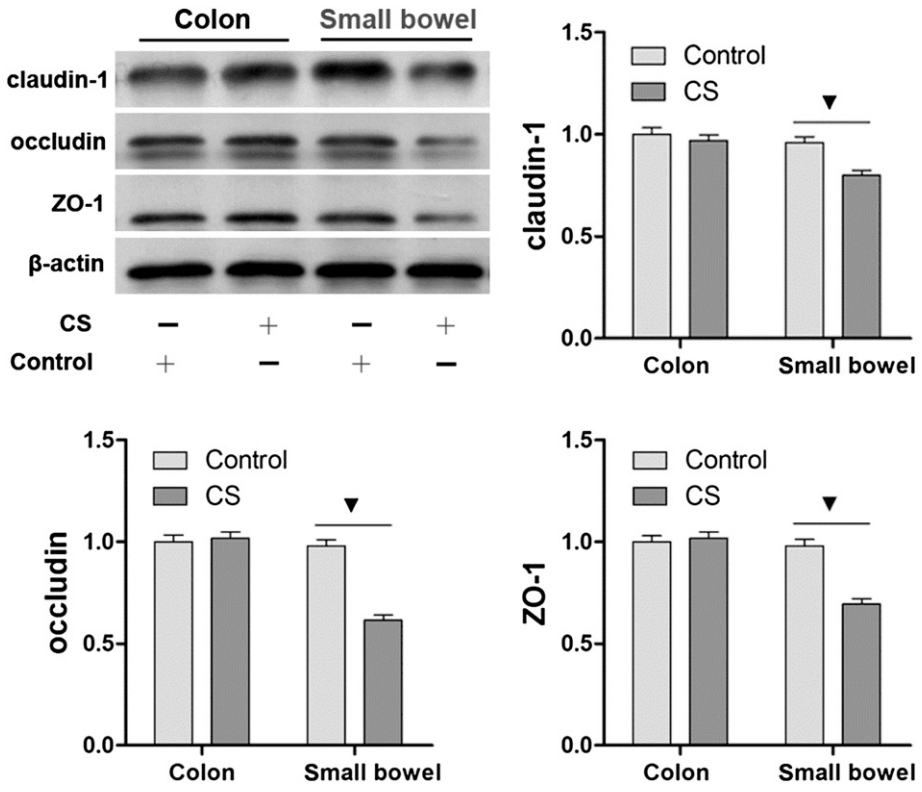

Figure 6 The concentration of claudin-1, occludin and ZO-1 in the small bowel mucosa of CS mice were found to be significantly lower compared to control mice. There was no significant difference in the colonic mucosa claudins between the two groups. Data are expressed as the mean ± SEM (n = 10 per group). $^{\blacktriangledown}P < 0.01$.

contribute to the intestinal barrier defect. TNF-α is known to induce an inflammatory response in intestinal epithelial cells [25], which we observed in the small bowel of CS mice in our study. Recent studies have also demonstrated that TNF-α impairs the intestinal TJ barrier through different mechanisms [26]. In intestinal Caco-2 cells, treatment with TNF-α increased inulin permeability, which may correlate with NF-κB activation based on the fact that inhibition of TNF-α-induced NF-κB activation by selected NF-κB inhibitors prevented the increase in TJ permeability in Caco-2 cells [27,28]. Tight junction proteins are known to contribute to barrier function and TJ structure. Low expression of ZO-1, occludin and claudin-1 was found in IL-10−/− mice and patients with IBD [29,30], and also in the small bowel of CS mice in our study. TNF-α can also reduce the expression of these tight junction proteins partly via the NF-κB pathway [26,29,31]. In addition, IL-1β plays an important role in the intestinal inflammatory process, and recent studies have shown that IL-β causes increased intestinal TJ permeability and that the IL-1β-induced decrease in tight junction protein expression may also be regulated by the NF-κB pathway [32–35]. HMGB1 can also be mediated by the NF-κB pathway [24] and increases the permeability of Caco-2 monolayers [36]. These studies indicated that the NF-κB signalling mediated cytokines can induce intestinal barrier defects [37]. This could partly explain the intestinal barrier dysfunction caused by CS exposure in our study.

Both clinical and animal research have demonstrated the protective role of CS in UC, which is an inflammatory disease involving the colon [38–40]. The adverse effects of CS on CD have also been fully confirmed [41,42]. However, the mechanisms involved in the opposite effects of smoking on CD and UC are only partially understood. Although several potential mechanisms, such as modulation of mucosal immune responses, and alterations in intestinal cytokine and eicosanoid levels have been proposed, none of these hypotheses could offer a satisfying explanation [43]. Unlike UC, CD can involve both the colon and small bowel. However, studies that compared the effect of smoking on CD did not focus on the effect of cigarette smoking on the location of the disease. To our best knowledge, no epidemiologic study directly addressed the question of the effect of smoking in patients with isolated Crohn's colitis. In fact, isolated Crohn's colitis is very rare and difficult to differentiate from UC [44,45]. This indicates that the small bowel may be the site of predilection of CD, although CD can affect the colon too. Combined with our interesting finding that, under the same CS stimulus, only the small bowel was involved, we have a reason to hypothesise that the opposite effects of smoking on UC and CD may be a consequence of the site of the disease (colon vs the small bowel) but not associated with a particular disease (UC vs CD). However, this finding needs further confirmation, especially, the observation of CS in isolated Crohn's colitis.

Stress may play an important role in the intestinal barrier dysfunction under CS exposure in our study. Stressors including hypoxic stress and psychological stress have been reported to be related to intestinal barrier dysfunction. CS mice in our study had a high level of carboxyhaemoglobin (air-exposed mice did not), which suggested CS mice might

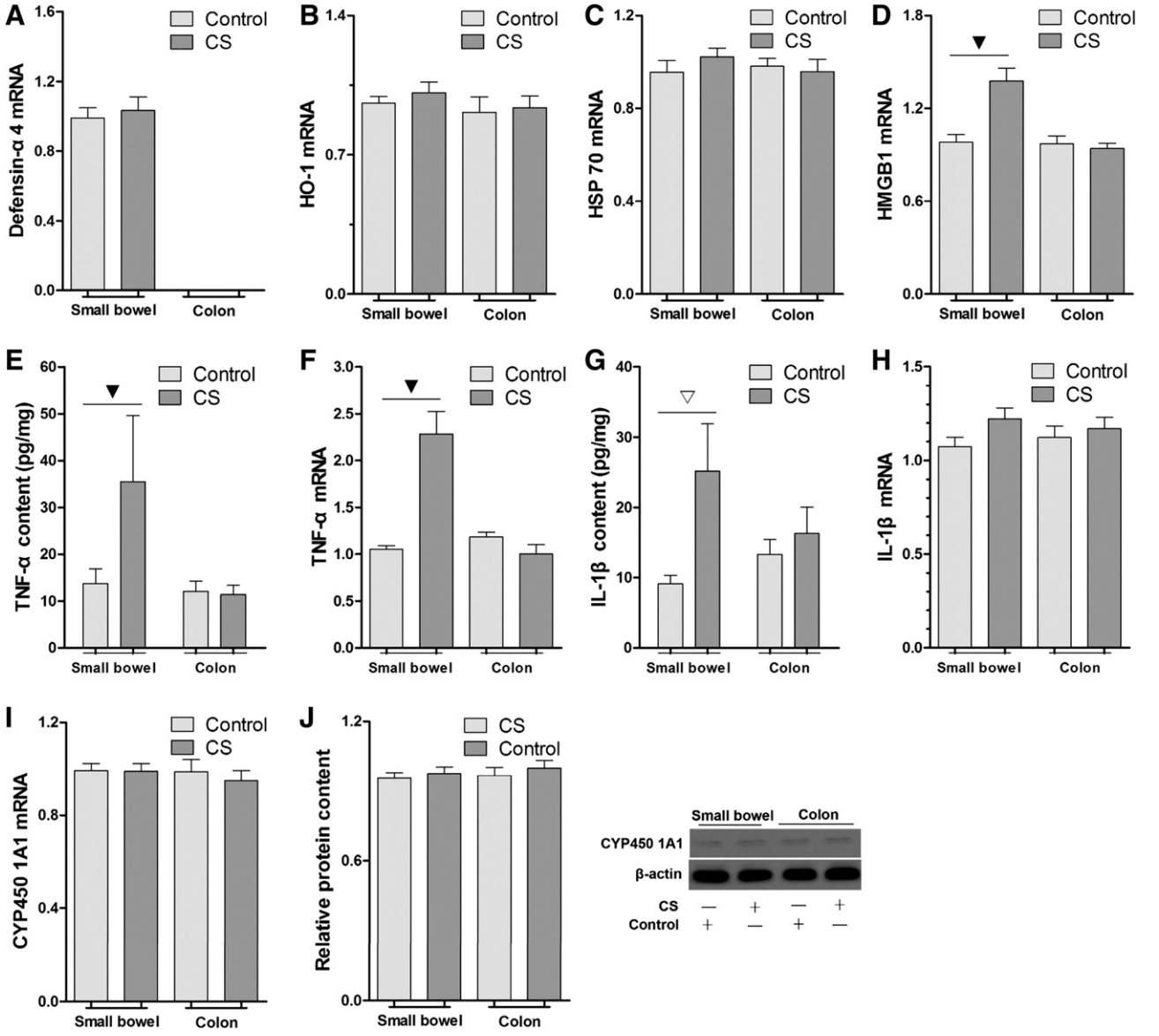

Figure 7 No significant difference was found when the mRNA expression of defensin-α4, HO-1 and HSP70 were compared between the two groups (A–C). The CS mice had a higher level of HMGB1 mRNA in small bowel than that of control group (D). CS exposure significantly elevated the concentration of TNF-α protein in the small bowel of CS mice compared to control mice (E), which was confirmed by assessing TNF-α mRNA expression (F). Concentration of IL-1β protein in the small bowel of CS mice were also found to be significantly increased compared with control mice (G); however, this finding was not confirmed by quantitative mRNA analysis (H; $P = 0.087$). There was no significant difference of CYP450 1A1 on the protein and mRNA level between the two groups (I, J). Data are expressed as the mean ± SEM (n = 10 per group). $^{\blacktriangledown}P < 0.01$; $^{\triangledown}P < 0.05$.

undergo hypoxia stress [46]. Several studies verified that hypoxemia can induce the intestinal barrier dysfunction. In a previous study, a single, 60-minute bout of moderate-to-high intensity exercise results in splanchnic hypoperfusion (decreases the supply of oxygen to the gut) and gut barrier dysfunction in healthy individuals [47]. Furthermore, this exercise-induced intestinal injury can be aggravated by ibuprofen (reducing perfusion within the splanchnic area) [48]. In addition, CS stimulation and hypoxia may induce psychological stress and result in the subsequent intestinal barrier dysfunction. Indeed, Cameron et al. found that mice under water avoidance stress developed increased permeability in the intestine [49]. Another work reported by Teitelbaum et al [50] indicated that corticotrophin-releasing factor (CRF, 50 μg/kg/day, delivered over 12 days via osmotic minipumps implanted subcutaneously) resulted in intestinal barrier dysfunction which was similar to that induced by psychological stress [49]. Therefore, further studies are needed to demonstrate whether CS exposure induced intestinal barrier dysfunction is associated with the stressors such as hypoxia and psychological stress.

The limitations in our study include: 1) we did not identify the exact element(s) in CS that can directly cause the changes in the intestinal barrier and inflammation, 2) although we found that intestinal barrier dysfunction could be caused by CS, which may occur via the NF-κB pathway,

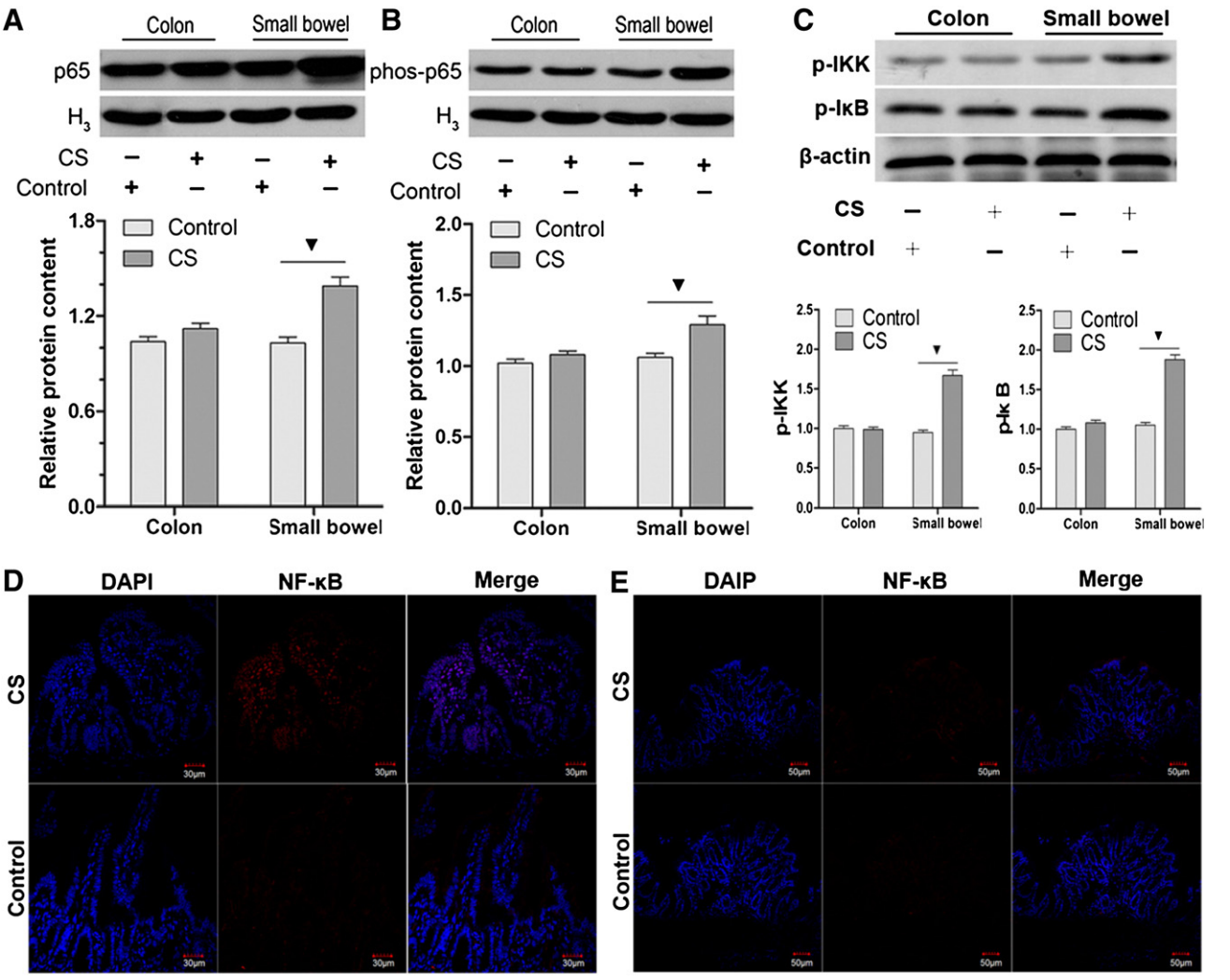

Figure 8 Both non-phosphorylated (A) and phosphorylated (B) forms of NF-κB p65 were increased in the small bowel of CS mice but there was no significant difference in NF-κB p65 in the colon of the two groups. The p-IKK and p-I κB were also found to be increased in the small bowel of CS mice (C). The subcellular localisation of NF-κB in the intestines of the two groups was determined (D, small bowel; E, colon). Detection of NF-κB in intestinal epithelial cells with antibody against NF-κB-p65. Red fluorescence indicates NF-κB. Blue fluorescence indicates the nuclei stained with DAPI. The pink colour results from the overlap of red-coloured NF-κB and blue-coloured nucleus. Data are expressed as the mean ± SEM (n = 10 per group). $^{\blacktriangledown}P < 0.01$.

other signalling pathways may be involved. In fact, tobacco smoke contains more than 4500 chemicals, many of them toxic or interfering with the immune system [51]. Among them, nicotine, carbon monoxide and nitrogen oxide are known to have immunomodulatory capacities and are possible mediators in the pathogenesis of IBD, but also other tobacco constituents can interact with intestinal immunity and gut function [52,53].

The strengths of our study are summarised as follows: 1) to our best knowledge, this is the first demonstration that the impact of CS on the intestinal barrier function exhibits organ specificity, which may be a helpful account for the dual effect of smoking on UC and CD; 2) we recommend the smoking mice model in our study, which exhibit several features of human IBD including malnutrition, increased intestinal permeability and inflammation. It can be used for research of IBD and intestinal barrier function, especially in small bowel diseases.

In conclusion, this study examined the effect of CS on both the small intestine and colonic intestinal barrier function in mice with no special genetic background or extraneous stimuli. We found that CS exposure could damage both the structure and function of intestinal barrier, based on the evidence that CS mice exhibited increased intestinal permeability, bacterial translocation, intestinal villi atrophy, damaged tight junctions and abnormal tight junction proteins. However, only the small bowel was affected. Our direct evidence demonstrates that the impact of CS on intestinal barrier function exhibits organ specificity, which may help to account for the opposite effects of smoking on CD and UC. Our finding also reminds us of the importance of the site of disease in the pathogenesis of IBD.

Conflict of interest

The authors declare that they have no conflicts of interests.

Acknowledgement

This work was supported partly by funding from the National Ministry of Health for the Digestive Disease (Grant 201002020) and National Natural Science Foundation of China (Grants 81200263 and 81170365).

References

1. Ananthakrishnan AN. Environmental triggers for inflammatory bowel disease. *Curr Gastroenterol Rep* 2013;**15**(1):302.
2. Lakatos PL, Szamosi T, Lakatos L. Smoking in inflammatory bowel diseases: good, bad or ugly. *World J Gastroenterol* 2007;**13**(46): 6134–9.
3. McGuckin MA, Eri R, Simms LA, Florin TH, Radford-Smith G. Intestinal barrier dysfunction in inflammatory bowel diseases. *Inflamm Bowel Dis* 2009;**15**(1):100–13.
4. Porras M, Martin MT, Yang PC, Jury J, Perdue MH, Vergara P. Correlation between cyclical epithelial barrier dysfunction and bacterial translocation in the relapses of intestinal inflammation. *Inflamm Bowel Dis* 2006;**12**(9):843–52.
5. Verschuere S, De Smet R, Allais L, Cuvelier CA. The effect of smoking on intestinal inflammation: what can be learned from animal models. *J Crohns Colitis* 2012;**6**(1):1–12.
6. Parkes GC, Whelan K, Lindsay JO. Smoking in inflammatory bowel disease: impact on disease course and insights into the aetiology of its effect. *J Crohns Colitis* 2014;**8**(8):717–25.
7. Prytz H, Benoni C, Tagesson C. Does smoking tighten the gut. *Scand J Gastroenterol* 1989;**24**(9):1084–8.
8. Suenaert P, Bulteel V, Den HE, Hiele M, Peeters M, Monsuur F, et al. The effects of smoking and indomethacin on small intestinal permeability. *Aliment Pharmacol Ther* 2000;**14**(6):819–22.
9. Benoni C, Prytz H. Effects of smoking on the urine excretion of oral 51Cr EDTA in ulcerative colitis. *Gut* 1998;**42**(5):656–8.
10. Braber S, Henricks PA, Nijkamp FP, Kraneveld AD, Folkerts G. Inflammatory changes in the airways of mice caused by cigarette smoke exposure are only partially reversed after smoking cessation. *Respir Res* 2010;**11**:99.
11. D'hulst AI, Vermaelen KY, Brusselle GG, Joos GF, Pauwels RA. Time course of cigarette smoke-induced pulmonary inflammation in mice. *Eur Respir J* 2005;**26**(2):204–13.
12. Verschuere S, Bracke KR, Demoor T, Plantinga M, Verbrugghe P, Ferdinande L, et al. Cigarette smoking alters epithelial apoptosis and immune composition in murine GALT. *Lab Invest* 2011;**91**(7): 1056–67.
13. Macdonald G, Kondor N, Yousefi V, Green A, Wong F, Aquino-Parsons C. Reduction of carboxyhaemoglobin levels in the venous blood of cigarette smokers following the administration of carbogen. *Radiother Oncol* 2004;**73**(3):367–71.
14. Muhammad-Kah RS, Hayden AD, Liang Q, Frost-Pineda K, Sarkar M. The relationship between nicotine dependence scores and biomarkers of exposure in adult cigarette smokers. *Regul Toxicol Pharmacol* 2011;**60**(1):79–83.
15. Gareau MG, Jury J, Perdue MH. Neonatal maternal separation of rat pups results in abnormal cholinergic regulation of epithelial permeability. *Am J Physiol Gastrointest Liver Physiol* 2007;**293**(1): G198–203.
16. Wang H, Zhang W, Zuo L, Zhu W, Wang B, Li Q, et al. Bifidobacteria may be beneficial to intestinal microbiota and reduction of bacterial translocation in mice following ischaemia and reperfusion injury. *Br J Nutr* 2013;**109**(11):1990–8.
17. Kosiewicz MM, Nast CC, Krishnan A, Rivera-Nieves J, Moskaluk CA, Matsumoto S, et al. Th-1type responses mediate spontaneous ileitis in a novel murine model of Crohn's disease. *J Clin Invest* 2001;**107**(6):695–702.
18. Wu LL, Chiu HD, Peng WH, Lin BR, Lu KS, Lu YZ, et al. Epithelial inducible nitric oxide synthase causes bacterial translocation by impairment of enterocytic tight junctions via intracellular signals of Rho-associated kinase and protein kinase C zeta. *Crit Care Med* 2011;**39**(9):2087–98.
19. Ke SZ, Ni XY, Zhang YH, Wang YN, Wu B, Gao FG. Camptothecin and cisplatin upregulate ABCG2 and MRP2 expression by activating the ATM/NF-kappaB pathway in lung cancer cells. *Int J Oncol* 2013;**42**(4):1289–96.
20. Di PNC, Tuve S, Ni S, Hellstrom KE, Hellstrom I, Lieber A. Effect of adenovirus-mediated heat shock protein expression and oncolysis in combination with low-dose cyclophosphamide treatment on antitumor immune responses. *Cancer Res* 2006;**66**(2):960–9.
21. Cheng YT, Wu SL, Ho CY, Huang SM, Cheng CL, Yen GC. Beneficial Effects of Camellia Oil (*Camellia oleifera Abel.*) on Ketoprofen-Induced Gastrointestinal Mucosal Damage through Upregulation of HO-1 and VEGF. *J Agric Food Chem* 2014 Jan 9 [Epub ahead of print].
22. Dong W, Zhang Z, Liu Z, Liu H, Wang X, Bi S, et al. Protective effects of osthole, a natural derivative of coumarin, against intestinal ischemia-reperfusion injury in mice. *Int J Mol Med* 2013;**31**(6):1367–74.
23. Stenman LK, Holma R, Eggert A, Korpela R. A novel mechanism for gut barrier dysfunction by dietary fat: epithelial disruption by hydrophobic bile acids. *Am J Physiol Gastrointest Liver Physiol* 2013;**304**(3):G227–34.
24. He ZW, Qin YH, Wang ZW, Chen Y, Shen Q, Dai SM. HMGB1 acts in synergy with lipopolysaccharide in activating rheumatoid synovial fibroblasts via p38 MAPK and NF-kappaB signaling pathways. *Mediators Inflamm* 2013;**2013**:596716.
25. Schulzke JD, BCheng YT, Wu SL, Ho CY, Huang SM, Cheng CL, Yen GC. Beneficial Effects of Camellia Oil (Camellia oleifera Abel.) on Ketoprofen-Induced Gastrointestinal Mucosal Damage through Upregulation of HO-1 and VEGF. J Agric Food Chem 2014 Jan 9 [Epub ahead of print].ojarski C, Zeissig S, Heller F, Gitter AH, Fromm M. Disrupted barrier function through epithelial cell apoptosis. *Ann N Y Acad Sci* 2006;**1072**:288–99.
26. Watson AJ, Hughes KR. TNF-alpha-induced intestinal epithelial cell shedding: implications for intestinal barrier function. *Ann N Y Acad Sci* 2012;**1258**:1–8.
27. Ma TY, Iwamoto GK, Hoa NT, Akotia V, Pedram A, Boivin MA, et al. TNF-alpha-induced increase in intestinal epithelial tight junction permeability requires NF-kappa B activation. *Am J Physiol Gastrointest Liver Physiol* 2004;**286**(3): G367–76.
28. Graham WV, Wang F, Clayburgh DR, Cheng JX, Yoon B, Wang Y, et al. Tumor necrosis factor-induced long myosin light chain kinase transcription is regulated by differentiation-dependent signaling events. *Characterization of the human long myosin light chain kinase promoter. J Biol Chem* 2006;**281**(36):26205–15.
29. Amasheh M, Fromm A, Krug SM, Amasheh S, Andres S, Zeitz M, et al. TNFalpha-induced and berberine-antagonized tight junction barrier impairment via tyrosine kinase, Akt and NFkappaB signaling. *J Cell Sci* 2010;**123**(Pt23):4145–55.
30. Chen HQ, Yang J, Zhang M, Zhou YK, Shen TY, Chu ZX, et al. Lactobacillus plantarum ameliorates colonic epithelial barrier dysfunction by modulating the apical junctional complex and PepT1 in IL-10 knockout mice. *Am J Physiol Gastrointest Liver Physiol* 2010;**299**(6):G1287–97.
31. Takahashi A, Kondoh M, Suzuki H, Watari A, Yagi K. Pathological changes in tight junctions and potential applications into therapies. *Drug Discov Today* 2012;**17**(13–14):727–32.

32. Barksby HE, Lea SR, Preshaw PM, Taylor JJ. The expanding family of interleukin-1 cytokines and their role in destructive inflammatory disorders. *Clin Exp Immunol* 2007;**149**(2):217–25.
33. Al-Sadi RM, Ma TY. IL-1beta causes an increase in intestinal epithelial tight junction permeability. *J Immunol* 2007;**178**(7):4641–9.
34. Al-Sadi R, Ye D, Dokladny K, Ma TY. Mechanism of IL-1beta-induced increase in intestinal epithelial tight junction permeability. *J Immunol* 2008;**180**(8):5653–61.
35. Al-Sadi R, Ye D, Said HM, Ma TY. IL-1beta-induced increase in intestinal epithelial tight junction permeability is mediated by MEKK-1 activation of canonical NF-kappaB pathway. *Am J Pathol* 2010;**177**(5):2310–22.
36. Sappington PL, Yang R, Yang H, Tracey KJ, Delude RL, Fink MP. HMGB1 B box increases the permeability of Caco-2 enterocytic monolayers and impairs intestinal barrier function in mice. *Gastroenterology* 2002;**123**(3):790–802.
37. Ye D, Ma I, Ma TY. Molecular mechanism of tumor necrosis factor-alpha modulation of intestinal epithelial tight junction barrier. *Am J Physiol Gastrointest Liver Physiol* 2006;**290**(3):G496–504.
38. Eliakim R, Karmeli F, Cohen P, Heyman SN, Rachmilewitz D. Dual effect of chronic nicotine administration: augmentation of jejunitis and amelioration of colitis induced by iodoacetamide in rats. *Int J Colorectal Dis* 2001;**16**(1):14–21.
39. Wang H, Zhao JX, Hu N, Ren J, Du M, Zhu MJ. Side-stream smoking reduces intestinal inflammation and increases expression of tight junction proteins. *World J Gastroenterol* 2012;**18**(18):2180–7.
40. van der Heide F, Dijkstra A, Weersma RK, Albersnagel FA, van der Logt EM, Faber KN, et al. Effects of active and passive smoking on disease course of Crohn's disease and ulcerative colitis. *Inflamm Bowel Dis* 2009;**15**(8):1199–207.
41. Kennelly RP, Subramaniam T, Egan LJ, Joyce MR. Smoking and Crohn's disease: active modification of an independent risk factor (education alone is not enough). *J Crohns Colitis* 2013;**7**(8):631–5.
42. Bergeron V, Grondin V, Rajca S, Maubert MA, Pigneur B, Thomas G, et al. Current smoking differentially affects blood mononuclear cells from patients with Crohn's disease and ulcerative colitis: relevance to its adverse role in the disease. *Inflamm Bowel Dis* 2012;**18**(6):1101–11.
43. Birrenbach T, Bocker U. Inflammatory bowel disease and smoking: a review of epidemiology, pathophysiology, and therapeutic implications. *Inflamm Bowel Dis* 2004;**10**(6):848–59.
44. Randell RL, Long MD, Cook SF, et al. Validation of an internet-based cohort of inflammatory bowel disease (CCFA partners). *Inflamm Bowel Dis* 2014;**20**(3):541–4.
45. Bressenot A, Geboes K, Vignaud JM, Gueant JL, Peyrin-Biroulet L. Microscopic features for initial diagnosis and disease activity evaluation in inflammatory bowel disease. *Inflamm Bowel Dis* 2013;**19**(8):1745–52.
46. Feiner JR, Rollins MD, Sall JW, Eilers H, Au P, Bickler PE. Accuracy of carboxyhemoglobin detection by pulse CO-oximetry during hypoxemia. *Anesth Analg* 2013;**117**(4):847–58.
47. van Wijck K, Lenaerts K, van Loon LJ, Peters WH, Buurman WA, Dejong CH. Exercise-induced splanchnic hypoperfusion results in gut dysfunction in healthy men. *PLoS One* 2011;**6**(7):e22366.
48. Van Wijck K, Lenaerts K, Van Bijnen AA, et al. Aggravation of exercise-induced intestinal injury by Ibuprofen in athletes. *Med Sci Sports Exerc* 2012;**44**(12):2257–62.
49. Cameron HL, Perdue MH. Stress impairs murine intestinal barrier function: improvement by glucagon-like peptide-2. *J Pharmacol Exp Ther* 2005;**314**(1):214–20.
50. Teitelbaum AA, Gareau MG, Jury J, Yang PC, Perdue MH. Chronic peripheral administration of corticotropin-releasing factor causes colonic barrier dysfunction similar to psychological stress. *Am J Physiol Gastrointest Liver Physiol* 2008;**295**(3):G452–9.
51. Rom O, Avezov K, Aizenbud D, Reznick AZ. Cigarette smoking and inflammation revisited. *Respir Physiol Neurobiol* 2013;**187**(1):5–10.
52. Mehta H, Nazzal K, Sadikot RT. Cigarette smoking and innate immunity. *Inflamm Res* 2008;**57**(11):497–503.
53. Leach PT, Cordero KA, Gould TJ. The effects of acute nicotine, chronic nicotine, and withdrawal from chronic nicotine on performance of a cued appetitive response. *Behav Neurosci* 2013;**127**(2):303–10.